Steel and Composite Structures, *Vol. 31, No. 5 (2019) 453-467*
DOI: https://doi.org/10.12989/scs.2019.31.5.453

Novel pin jointed moment connection for cold-formed steel trusses

Chris Mathison [1a], Krishanu Roy [*2], G. Charles Clifton [2b],
Amin Ahmadi [2c], Rehan Masood [2,3d] and James B.P. Lim [2e]

[1] *Holmes Consulting LP, Auckland, New Zealand*
[2] *Department of Civil and Environmental Engineering, The University of Auckland, Auckland, New Zealand*
[3] *Department of Construction Engineering & Management, NIT-SCEE,*
National University of Science and Technology, H-12, Islamabad, Pakistan

(*Received December 18, 2018, Revised April 22, 2019, Accepted April 24, 2019*)

Abstract. Portal frame structures, made up of cold-formed steel trusses, are increasingly being used for lightweight building construction. A novel pin-jointed moment connector, called the Howick Rivet Connector (HRC), was developed and tested previously in T-joints and truss assemblage to determine its reliable strength, stiffness and moment resisting capacity. This paper presents an experimental study on the HRC, in moment resisting cold-formed steel trusses. The connection method is devised where intersecting truss members are confined by a gusset connected by HRCs to create a rigid moment connection. In total, three large scale experiments were conducted to determine the elastic capacity and cyclic behaviour of the gusseted truss moment connection comprising HRC connectors. Theoretical failure loads were also calculated and compared against the experimental failure loads. Results show that the HRCs work effectively at carrying high shear loads between the members of the truss, enabling rigid behaviour to be developed and giving elastic behaviour without tilting up to a defined yield point. An extended gusset connection has been proposed to maximize the moment carrying capacity in a truss knee connection using the HRCs, in which they are aligned around the perimeter of the gusset to maximize the moment capacity and to increase the stability of the truss knee joint.

Keywords: cold-formed steel; novel connection; moment connection; pinned joint; HRC

1. Introduction

Cold-formed steel (CFS) is becoming increasingly popular in the building industry, due to its dimensional stability, high strength to weight ratio and ease of formability into a wide range of structural components (Darcy and Mahendran 2008, Roy *et al*. 2018a-c, 2019, Ting *et al*. 2018). Specifically, CFS trusses are widely used in portal frames and lightweight floors joists. Single channel or back-to-back channel sections are used as chord and web members, connected with bolts or screws, to transfer axial forces to other members through shear in the connector.

However, the connectors in the CFS trusses causes around 40% of the total cost of the construction for long span portal frames, which is quite uneconomical. Furthermore, to transfer the significant bending moment at the knee and apex joints from portal frame type buildings, large numbers of screw connectors are required because each screw connector has low shear strength and proportionality limit (end of the initial elastic range under load). This also limits the maximum span to be achieved economically to around 25 m. High loading applications can be achieved with bolts being used as connector elements. However, there are limitations to contact plies, which is not suited for CFS portal frames. There is high tearing (failure) of solid bolt than thin gauge steel element and slip due to predrilling of bolt holes reducing stiffness in moment connections unless the bolts are fully tensioned which is not typical practice (Lim and Nethercot 2004). Many different configurations of CFS connections are available, which includes self-piercing rivets; press joining and the Rosette tube joint (Kaitila *et al*. 2001).

Common types of rigid connections used in industry are bolted endplate connection, mitred connection, back-to-back bolted connection and screw connections, gusseted connection and braced connection (see Fig. 1). The bolted endplate connection is similar to hot-rolled steel connections and is among the most commonly used CFS connections in low span sheds. Mills (2012) conducted several tests on this connection checking different variables and variations. He concluded that this connection consistently underperforms and therefore, not recommended for thin gauge CFS sections. On the other hand, mitred joint is not commonly used in CFS portal frames because of low constructional tolerances and difficulty in maintaining stability of the joint against twist under negative moment

∗Corresponding author, Ph.D. Candidate,
E-mail: kroy405@aucklanduni.ac.nz
[a] Structural Engineer,
E-mail: chrismathieson@holmesgroup.com
[b] Associate Professor, E-mail: c.clifton@auckland.ac.nz
[c] Ph.D. Candidate, E-mail: aahm810@aucklanduni.ac.nz
[d] Ph.D. Candidate, E-mail: rehan.masood@auckland.ac.nz
[e] Associate Professor, E-mail: james.lim@auckland.ac.nz

http://www.techno-press.org/?journal=scs&subpage=6
ISSN: 1229-9367 (Print), 1598-6233 (Online)

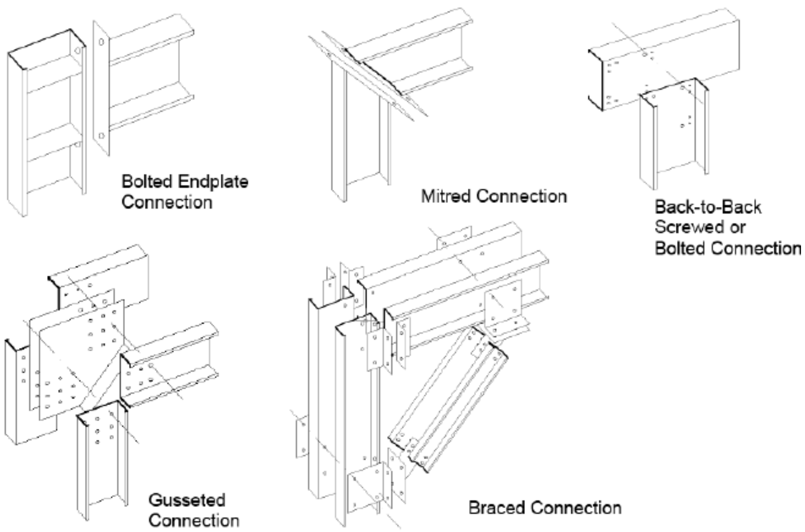

Fig. 1 Common CFS portal frame moment connections (Wrzesien et al. 2012)

(Mills and Laboube 2004). Mills (2000) proposed back-to-back screwed connections in CFS structures. The main issue regarding this connection is aesthetical, however the intended purpose is for sheds. Dundu (2011) created a guideline for designing 10-12 m span portal frames using bolts instead of screws. Other works include that of Li *et al*. (2017), who investigated the failure modes, initial stiffness and bending moment capacities of embedded column base connection, also propose analytical model for design purpose. For other composite structural elements such as concrete filled steel tubes (beam-column connection), semi-rigid connections were found to be effective (Beena *et al*. 2017). On the other hand, Nunez *et al*. (2017) investigated the seismic performance of moment connections in steel moment frames with HSS columns.

Common types of rigid connections used in industry are bolted endplate connection, mitred connection, back-to-back bolted connection and screw connections, gusseted connection and braced connection (see Fig. 1). The bolted endplate connection is similar to hot-rolled steel connections and is among the most commonly used CFS connections in low span sheds. Mills (2012) conducted several tests on this connection checking different variables and variations. He concluded that this connection consistently underperforms and therefore, not recommended for thin gauge CFS sections. On the other hand, mitred joint is not commonly used in CFS portal frames because of low constructional tolerances and difficulty in maintaining stability of the joint against twist under negative moment (Mills and Laboube 2004). Mills (2000) proposed back-to-back screwed connections in CFS structures. The main issue regarding this connection is aesthetical, however the intended purpose is for sheds. Dundu (2011) created a guideline for designing 10-12 m span portal frames using bolts instead of screws. Other works include that of Li *et al*. (2017), who investigated the failure modes, initial stiffness and bending moment capacities of embedded column base connection, also propose analytical model for design purpose. For other composite structural elements such as concrete filled steel tubes (beam-column connection), semi-rigid connections were found to be effective (Beena *et al*. 2017). On the other hand, Nunez *et al*. (2017) investigated the seismic performance of moment connections in steel moment frames with HSS columns.

In terms of gusseted connections, having many forms and benefits. For large span portal frames, it is usually desirable to have double C-sections connected back-to-back to increase their load carrying capacity. Symmetric connections with gussets placed inside are suitable and convenient in this arrangement as buckling due to asymmetry is largely eliminated. It has been shown that the strength of the gusset can be controlled so that failure occurs outside the connection allowing for the full capacity of the connected members to be utilized (Wrzesien *et al*. 2012). It should be noted that the use of gussets in most contexts allows two separate members to be connected in-plane when overlap of these members is not possible. In this case, the gusset acts as an intermediate between the two members, transferring moment and shear across the connection. This system has been used in New Zealand on spans of up to 30 metres.

On the other hand, knee braces can be an inexpensive alternative to connections as it creates a deep lever arm in the moment resisting corner, thereby allowing increased capacity and stiffness compared to connections limited to the depth of the adjoining members. One downside to this method is that the clear height to the eves of the portal frame is significantly reduced (Wrzesien *et al*. 2012); this would be even more of an issue with trusses, which are deeper members than solid web C-sections.

In New Zealand, a new form of CFS connector, called The HRC (see Fig. 2), has been conceptualized and developed by Howick Ltd a New Zealand manufacturer of cold-formed systems and cold-forming machinery. It has been developed with objective to overcome two problems commonly associated with CFS connections; a low proportionality limit due to slip, tilting or bearing, and limited post peak strength and stiffness. The Howick Rivet Connector (HRC) has been increasingly used in past few years as connector elements in CFS trusses and T-joints.

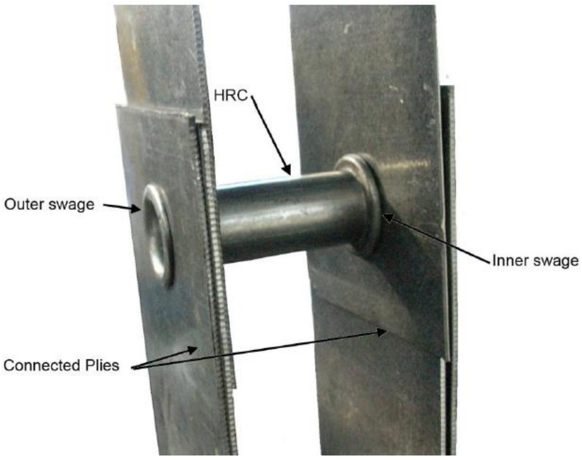

Fig. 2 Photograph of the Howick Rivet Connector (HRC)

The HRC comprises a galvanized hollow rivet that connects web and chord channel sections through their flanges by clamping them between an inner and outer swage (see Fig. 2). It has several advantages such as simple and short installation process, high post yielding ductility because of less use of steel within same diameter, no slip due to tight fit of rivet shank, and no tilting because of symmetry of connections.

Mathieson *et al*. (2016) investigated the performance and capacity of connections comprising HRC for T-joint and truss assembly, reporting both experiments and finite element analysis. Experimental results agreed well with the stiffness and strength, determined from theoretical equations. Ahmadi *et al*. (2016) conducted laboratory tests on twenty-seven HRC Tee-stub specimens; for comparison, another twenty-seven bolted Tee-stub specimens were also tested. In the laboratory tests, three different thicknesses of channel-sections and three different end distances were considered. It was concluded that the behaviour of the HRC Tee-stubs is similar to that of the bolted Tee-stubs, but the use of the HRC results in a higher capacity and an improved ductility. Design equations have also been proposed to predict the bearing strength of the HRC Tee-stubs by Ahmadi *et al*. (2016). This paper extends the work of Mathieson *et al*. (2016) and Ahmadi *et al*. (2016) to investigate the behaviour of moment connection based on intersecting truss members comprising HRC connectors. A connection method is devised where intersecting truss members are confined by a gusset connected by HRCs to create a rigid moment connection. Rigid connections in CFS structures have the greatest application in portal frames where the apex and knee are required to transfer vertical and horizontal forces acting on the structure in bending to connected columns and rafters. In this paper, three large scale experiments are reported which were conducted on the gusseted truss moment connection comprising HRC connectors (see Fig. 3). The moment connections were tested in a perpendicular arrangement to allow for the greatest moment to shear or axial force ratio to be developed. Theoretical failure loads were also calculated and compared against the experimental failure loads and finely the accuracy of the current design guidelines was checked for such moment connections comprising of HRCs in CFS trusses. The behaviour of HRCs in T-joints and trusses are also reported in this paper.

2. Experimental investigations

HRC has been previously investigated by Mathieson *et al*. (2016) for CFS T-joints and truss members. They have reported 39 tests on T-joint and 8 tests on CFS truss assembly. A summary of test results reported by Mathieson *et al*. (2016) is shown in Tables 1 and 2 for T-joint and truss

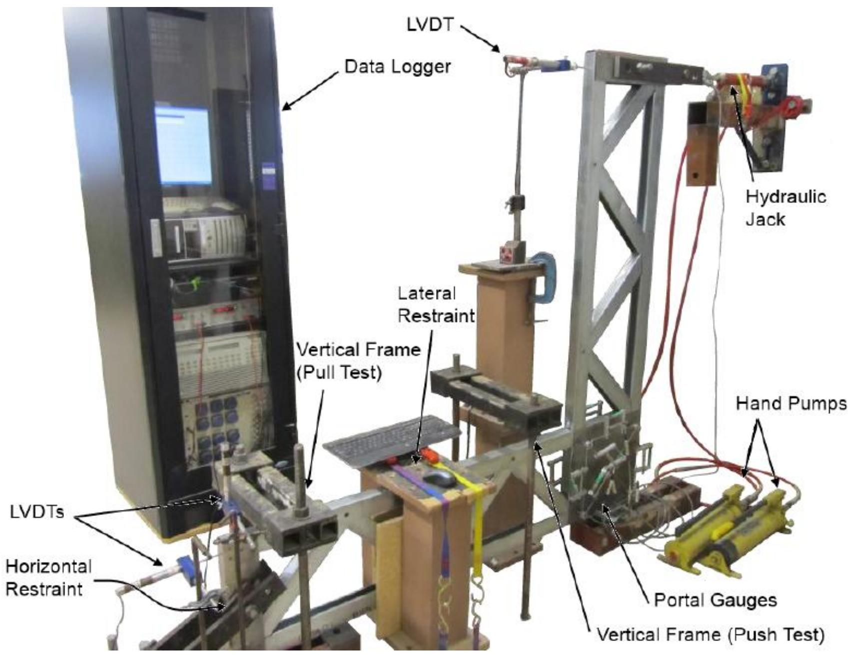

Fig. 3 Moment connection experimental setup

Table 1 T-joint test results

Rivet size	Member thickness (mm)	Average peak load (kN)	Standard deviation (kN)	Failure mode
12.7 × 0.95 mm	0.75	12.31	1.12	Bearing
	0.95	15.76	0.74	Shear
	1.15	15.81	0.60	Shear
12.7 × 1.55 mm	0.75	10.81	0.17	Bearing
	0.95	16.54	0.68	Bearing
	1.15	20.68	0.44	Bearing
15.9 × 1.15 mm	0.75	13.34	0.20	Bearing
	0.95	17.98	0.56	Bearing
	1.15	21.90	0.63	Bearing
31.8 × 1.85 mm	1.6	72.58	0.77	Bearing/Shear
	1.85	49.35	4.33	Bearing
	2.5	74.50	0.6	Shear
	3.0	76.12	1.2	Shear

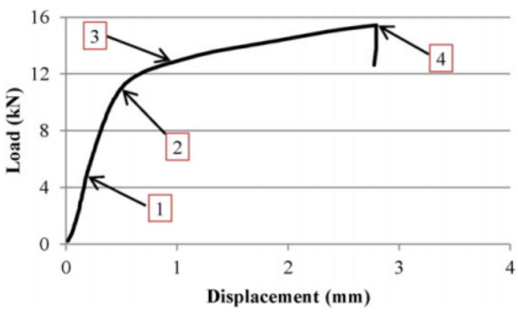

Fig. 4 T-joint test which underwent shear failure (0.95 mm member; 12.7 × 0.95 mm HRC)

*Note: displacement is the movement of the vertical stem of the tee relative to the horizontal stem of the tee, taken as the average of the measurements from each side

assembly, respectively. The load-displacement behaviour of specimen “0.95 mm member; 12.7 × 0.95 mm HRC” and “0.95 mm member; 15.9 × 1.15 mm HRC” is also shown in Figs. 4 and 5, respectively. As shown in Fig. 4, the T-joint (0.95 mm member; 12.7 × 0.95 mm HRC) underwent shear failure with stages defined and explained as follows:

(1) Elastic range - the HRC and connected plies are acting elastically (see Fig. 4)
(2) Rivet softening - the HRC starts to become inelastic and form plastic hinges; the plies do not undergo out of plane buckling.
(3) Rivet squashing - the HRC continues to squash into an oval shape with plastic hinges fully formed. Plies are stable while the load slowly increases to the peak load prior to the HRC rupturing.
(4) Ultimate failure - the HRC ruptures.

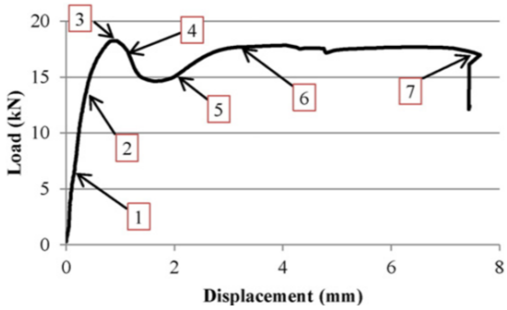

Fig. 5 T-joint test which underwent bearing failure (0.95 mm member; 15.9 × 1.15 mm HRC)

*Note: displacement is the movement of the vertical stem of the tee relative to the horizontal stem of the tee, taken as the average of the measurements from each side

A typical T-joint (0.95 mm member; 15.9 × 1.15 mm HRC) which underwent bearing failure is shown in Fig. 5 with stages defined and explained as follows:

(1) Elastic range - the HRC and connected plies are acting elastically, with the end of the elastic range referred to as the proportionality limit.
(2) Onset of bearing failure - the plies that are bearing on the HRC start to yield/deform out-of-plane as the bearing surface becomes inelastic and the rivet hole begins to extend.
(3) Peak load -the highest load reached.
(4) Buckling - the failed member buckles significantly out-of-plane.
(5) Ply bearing and work hardening - the failed member utilizes the bearing area gained by folding onto the swages while work hardening.
(6) Inelastic redistribution - as the buckled ply continues to work harden, redistribution of stresses around the rivet hole occurs.
(7) Ultimate failure - one or both sets of plies rupture.

An example of a T-joint specimen which failed in bearing is shown in Fig. 6. Similarly, in Fig. 7, the failure mode of a typical T-joint test specimen which failed in shear is shown.

On the other hand, the trusses tested were connected with 12.7 × 0.95 mm HRCs using 65 × 45 mm members, 0.75 mm and 0.95 mm thick, as these resulted in bearing

Table 2 Results of truss tests

Member thickness (mm)	Average peak load (kN)	Standard deviation (kN)	Failure mode	Expected peak load based on T-joint tests (kN)	Difference between actual and expected
0.75	10.78	2.04	Bearing	10.17 kN	6%
0.95	19.68	0.42	Shear	13.02 kN	51%

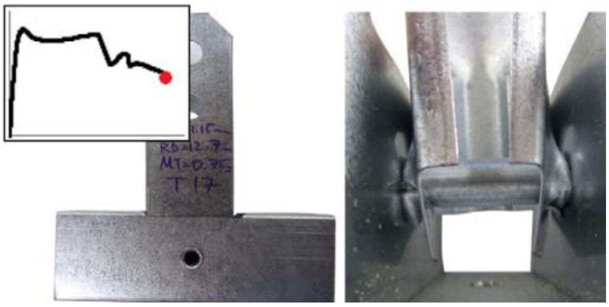

Fig. 6 Example of HRC bearing failure (0.75 mm member; 12.7 × 0.95 mm HRC)

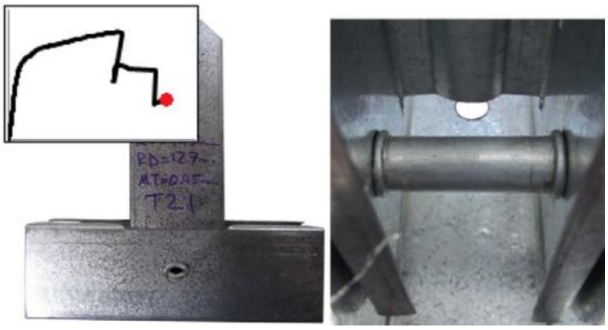

Fig. 7 Example of HRC shear failure (0.95 mm member; 12.7 × 0.95 mm HRC)

and shear failure modes respectively, in the T-joint tests. Four different types of truss were tested (8 tests in total). In Fig. 8, typical load-displacement curves of HRC in truss assembly are shown. Figs. 9 and 10 show the example of bearing failure and shear failure of HRC in truss assembly, respectively.

Ahmadi *et al*. (2016) also investigated the failure behaviour of HRC Tee-stub, with 27 test specimens with three different thicknesses i.e., 0.75 mm, 0.95 mm and 1.15 mm thickness of channel sections. Results from this study showed similar failure modes of HRC in T-joints as reported by Mathieson *et al*. (2016). Fig. 11 shows the failure models of Tee-stubs. As can be seen, 0.75 mm thick specimen had good ductility with higher yield strength. However, 0.95 mm thick specimen showed both bearing/

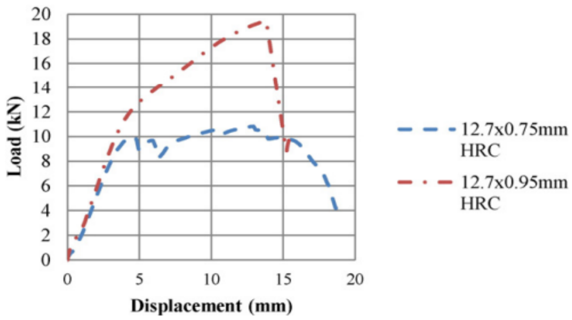

Fig. 8 Load-displacement curves of HRC in truss assembly

*Note: the blue line is bearing failure; red line is shear failure

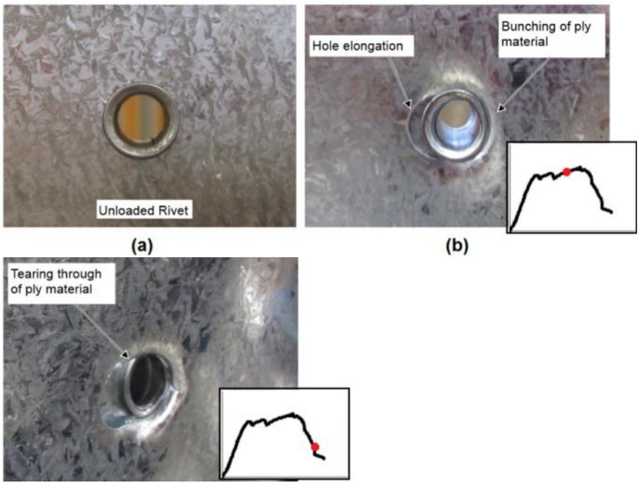

Fig. 9 Bearing failure sequence around HRC in truss assembly

tearing failure and shear failure simultaneously. Further, 1.15 mm thick specimen, failed mostly because of the shear failure of HRCs.

In order to understand the applicability of HRC in gusseted truss moment connections, three large scale experiments were conducted and reported in this paper. The gusseted truss moment connection and experimental setup is also presented in this section. The regime for testing was made on a test-by-test basis, depending on the performance of preceding tests and is presented accordingly in section 4. Figs. 2 and 3 shows the specimen used and test arrangement respectively. The details of the experimental investigation are described in the following sections.

2.1 Moment connection specimen

A non-braced moment connection using interconnecting truss members with gusset plates either side was tested. A connection where the truss members interconnect allows for a single group of HRCs, so that the strength and stiffness can be determined easily. Gusset plates act by transfeming

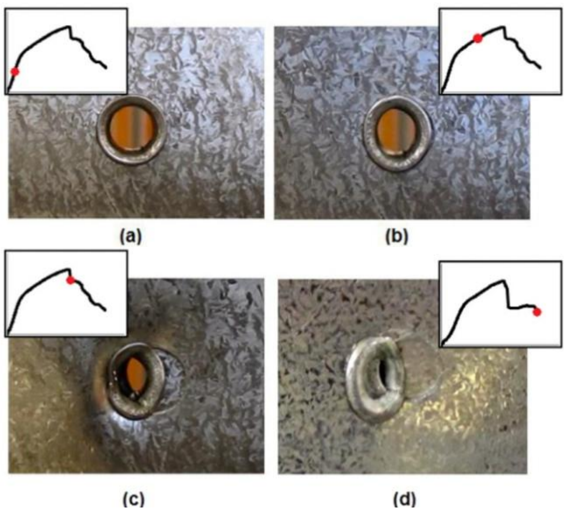

Fig. 10 Shear failure sequence for HRC in truss assembly

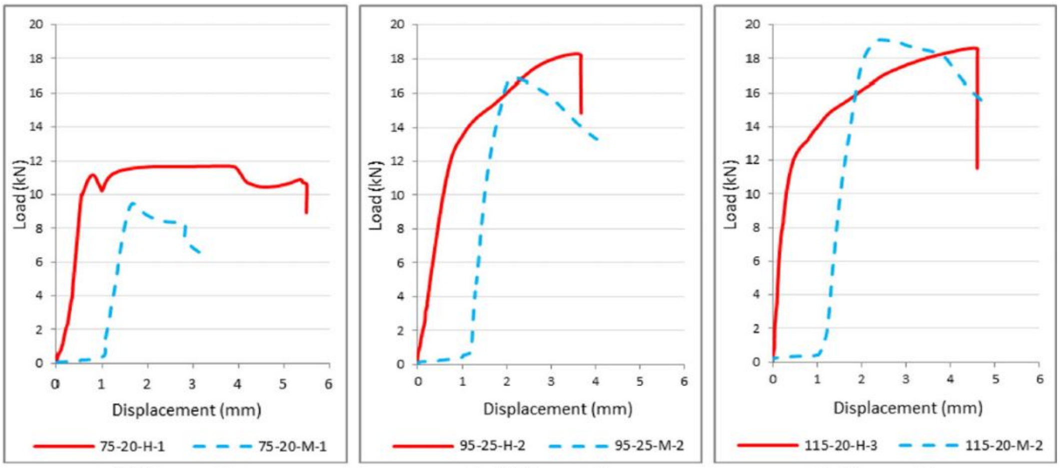

a. 0.75 mm plies b. 0.95 mm plies c. 1.15 mm plies

Fig. 11 Variation of load against displacement for HRC and bolted Tee-stubs

forces through panel shear as illustrated in Fig. 12. Without these panels, additional members must be introduced into the connection to carry internal diagonal actions. This poses two problems: the first being that the number of intersecting members decreases the constructability when installing HRCs, but more importantly a significant force concentration develops, placing significant stress on a single critical connector. A gusseted connection was therefore created for a non-braced truss portal frame with HRCs.

In order to create a relatively realistic test specimen, a suitable spanned portal frame was calculated using 65 × 45 × 0.95 mm lipped C-sections. The length of the specimen was determined from the approximate length to the point of contra flexure from the knee in the calculated frame. The point of contra flexure was used because a point load applied at one end of the specimen will make a similar loading distribution to that which would be expected in a vertically loaded portal frame. The floor trusses used as the frame members were 400 mm deep and 6.6 m long.

2.2 Applied load and moments

The loads applied to the trusses are summarized in Table 3 and reflect standard residential loads. The design load cases are 1.2G + 1.5Q for the ultimate limit state (ULS) and G + ψ_sQ (where ψ_s = 0.7 for short term loading) for the serviceability limit state (SLS) taken from AS/NZS1170.1 (2002). Note that if this were a non-trafficable roof of the building, ψ_s = 0 would apply. The permanent loads are assumed based on design experience and the imposed loads are for self-contained dwellings taken from AS/NZS1170.1 (2002) (see Table 3).

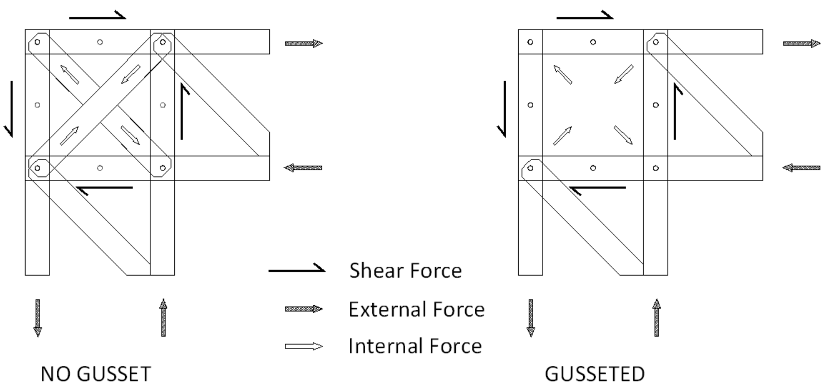

Fig. 12 Gusseted connection and connection using internal members

Table 3 Applied loads on trusses

Load case	Action	Stress (kPa)	Applied load (kN/m)
Permanent, G	Self-weight of truss and floor partitions	0.30	0.18
Imposed, Q	Self-contained dwelling in general areas	0.50	0.30
ULS, 1.2G+1.5Q	-	1.50	1.93
SLS, G+0.7Q	-	-	0.84

The moment generated for a 400 mm deep and 6.6 m long, floor truss was used as a starting point for a preliminary estimate on the span of the portal frame because this truss was at its load carrying capacity and was governed by the strength of the chords, which is proportional to the moment carried. M_{floor} is the moment resisted by this floor truss and calculated as 10.5 kNm with ω_{floor} as 1.93 kN/m and L_{floor} as 6.6 m.

$$M_{floor} = \frac{\omega_{floor} \ x \ L_{floor}{}^{2}}{8} \tag{1}$$

An estimate of the bending moment at the knee of a standard sized portal frame, M_{knee} under gravity loading was calculated as

$$M_{knee} = \frac{\omega_{portal} \ x \ L_{portal}{}^{2}}{16} \tag{2}$$

The assumed loads on the portal frame rafter are summarized in Table 4 based on a design load case of 1.2G + 1.5Q for ULS vertical loading from AS/NZS1170.0 (2002). A portal frame bay spacing of 3 m was considered.

Table 4 Applied loads on portal frame rafter

Load case	Action	Stress (kPa)	Applied load (kN/m)
Permanent, G	Self-weight of truss and roof	0.4	1.2
Imposed, Q	Other roofs	0.25	0.75
ULS, 1.2G + 1.5Q	-	-	2.57

By substituting M_{floor} equal to M_{knee} and rearranging Eq. (2), the assumed maximum portal span, L_{portal} was calculated as shown below in Eq. (3)

$$L_{portal} = \sqrt{\left(16 \ x \frac{10.5}{2.57}\right)} = 8.1 \text{ m} \tag{3}$$

If the point to contra flexure is at 20% of the portal frame span, the length of the specimen was about 1.6 m. Assuming this moment acts at the center of the gusset, a specimen length of around 1.8 m was chosen as shown in Fig. 13.

2.3 Moment connection details

The web members were placed at angles of 45 degrees and the rivets were equally spaced. The truss members had their webs cut where applicable to allow intersecting members through (see Fig. 13). A total of eight HRCs were used inside the connection because the internal capacity was a focus of this section and would likely be too strong to assess the capacity if more were put in. The ends of the specimen were made essentially rigid and had a large rivet installed which allowed a suitable sized bolt through. This bolt was sleeved in a steel pipe to make a snug fit (see Figs. 13 and 14).

2.4 Experimental setup

The moment connection specimen was loaded at 90 degrees to the actual plane of the specimen. As the purpose of this investigation was to assess the strength and stiffness of the moment connection rather than verifying an existing

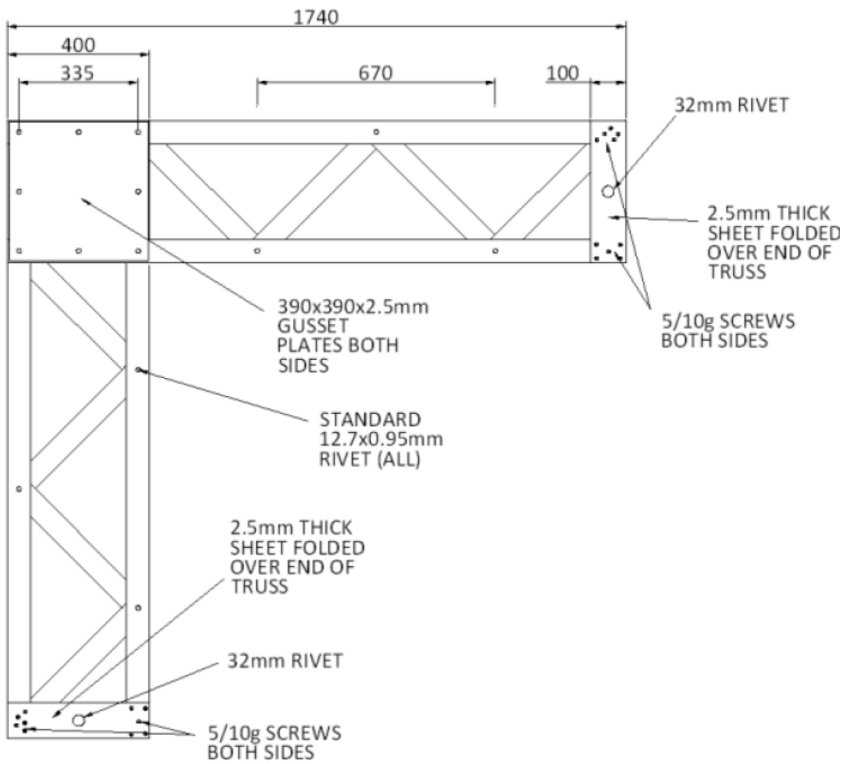

Fig. 13 Dimensions of moment connection specimen

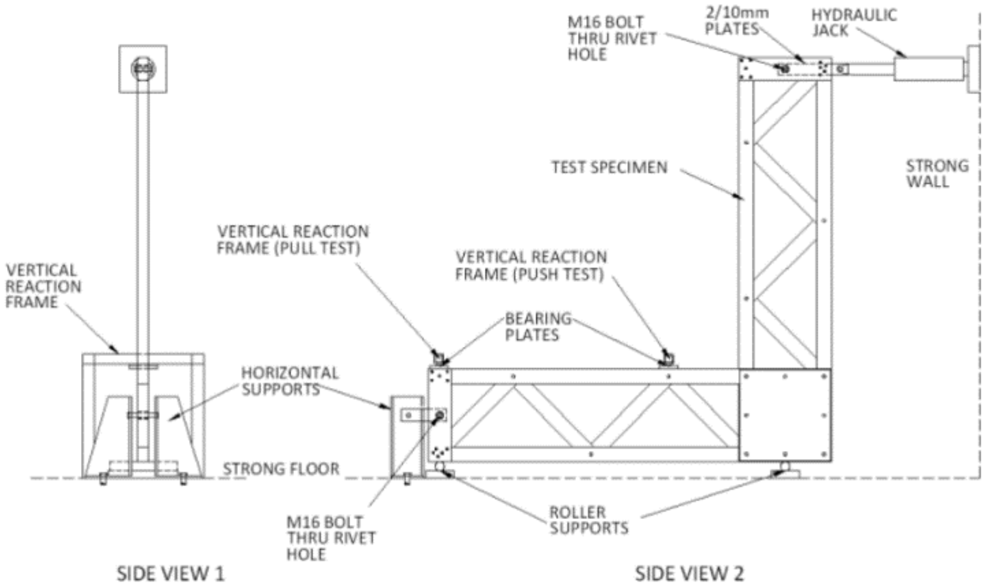

Fig. 14 Experimental setup for moment connection

connection method, it is advantageous to load the connection orthogonally as this produces the highest moment to shear or axial ratio. The experimental setup used is illustrated in Figs. 3 and 14.

A small hydraulic jack operated by a hand pump was used to push and pull the specimen from a strong wall. The roller supports and vertical reaction frames provided resistance to overturning and the horizontal support provided support against sliding. A lateral support, which consisted of timber boards, resting shy of the truss between two heavy steel box sections, was used.

Three LVDTs were used to measure the vertical and horizontal deflection of the truss. One was positioned at the top to measure the displacement of the jack and the other two were set up at the horizontal support to measure the relative horizontal displacement and vertical displacement at the end. An array of six portal gauges was set up on both sides of the gusset plate as shown in Fig. 15. The portal gauges were set up to measure the displacement between corners of the plate. It should be noted that the base plates were upturned before testing, allowing pinned rotation at the base of the specimen.

3. Test results and discussion

In this section the results from testing are presented and discussed in three parts, as the regime of testing for each specimen was determined based on the results from preceding tests. The theoretical loads acting through various components during loading are then, compared and discussed. An opening moment is caused by pulling the jack and is recorded as a positive load and displacement. Conversely, a closing moment was taken as negative in sign. The loads measured were converted to moments by multiplying the applied force by a factor of 1.49, which corresponds to the distance from the height of the applied load to the center of the gusset. The displacements measured at the top of the specimen (reduced by the base horizontal displacements) were converted to rotations, relative to the center of the gusset.

3.1 Test 1 (*Elastic capacity of the connection*)

The objective of the first test was to determine the elastic capacity of the connection in both an opening and

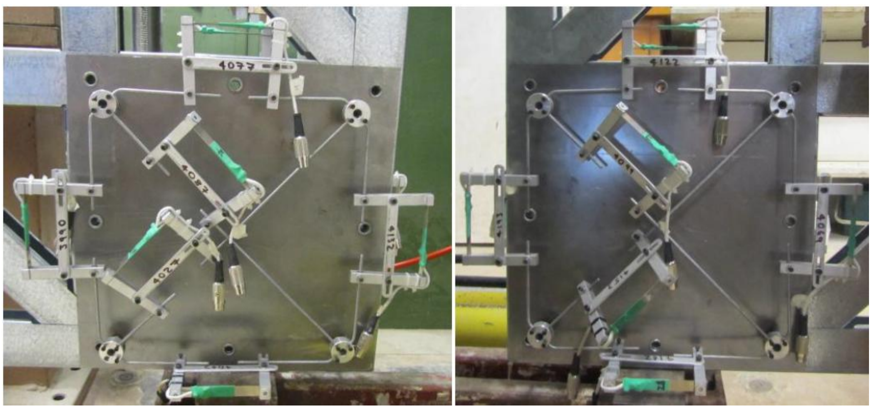

Fig. 15 Portal gauge arrangement on front and back of gusset plate

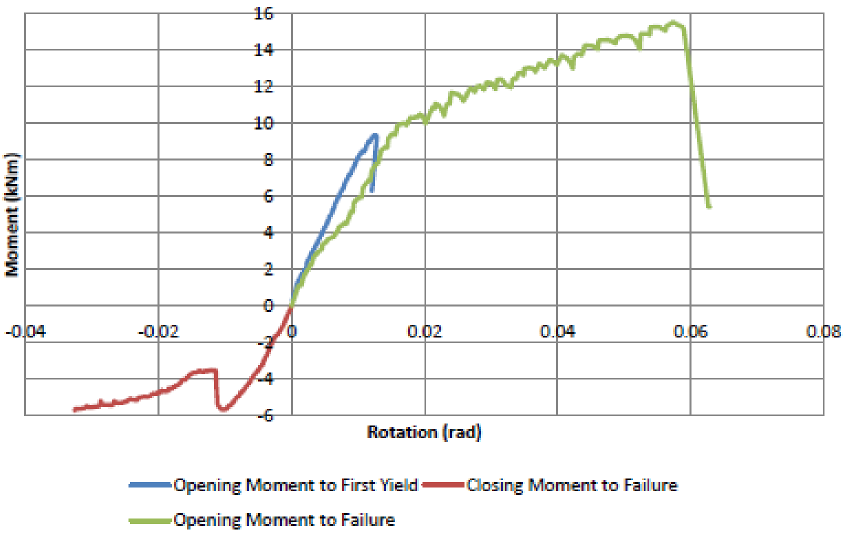

Fig. 16 First moment connection test result

closing moment. The results from the first test are plotted in Fig. 16. The specimen was firstly loaded in an opening moment to 9.3 kNm before the plot began to appear non-linear then the load was released back to origin. At a load of 3 kN, a small amount of distortional buckling in the lattice members was observed.

In the second stage of the test, the specimen was loaded in a closing (negative) moment, putting the inside chords into compression. At a moment of 3 kNm, a small amount of local buckling was observed in the inside chords near the gussets at the riveted area where the lips of the member had been cut. At a moment of 4.5 kNm, lateral restraint was required to hold the vertical truss against global sideways buckling of the truss.

Failure of the compression chord occurred at a load of -5.7 kNm where the lips and web members had been cut to allow intersecting members through. The flanges buckled sideways until the uncut web began to bear against the intersecting chord web (see Fig. 17). The load was increased until it was noticed that progressive tearing of the member was occurring along the web to flange intersection.

In the final stage of loading, the specimen was subjected to an opening (positive) moment until failure occurred. There was a small amount of initial slip due to tension of the inner chord member straightening out of the squashed portion of the specimen. The damage due to sideways buckling was seen not to affect the capacity of the member as long as net section failure did not occur at the damaged portion. The rivets outside the gusseted connection all began to squash simultaneously before the rivet closest to gusseted connection in the bottom truss fractured at a moment of 15.5 kNm. Fig. 18 shows the failed specimen highlighting the rivet which ultimately failed, though it should be noted that all other rivets outside the gusset were also on the verge of fracture. Also shown in Fig. 18, is the web buckling of compression member just outside the gusset. The degree of buckling at this section increased significantly when the rivets began to soften because the truss members became increasingly flexible while the gusseted connection remained rigid.

The forces in each of the members of the specimen relative to a nominal force, P of 100 units applied at the top was calculated using force equilibrium and is shown in Fig. 19. It can be seen that the maximum force in the chords is equal to 4 P adjacent to the gusseted connection, the forces in the webs are constant at 1.41 P and the maximum force acting through each connector is constant and equal to 2 P. The constant force applied to each connection is why the rivets were all observed to fail simultaneously. Fig. 20 shows the relative force vectors acting on the HRCs within

Fig. 17 Sideways buckling failure of the compression chord

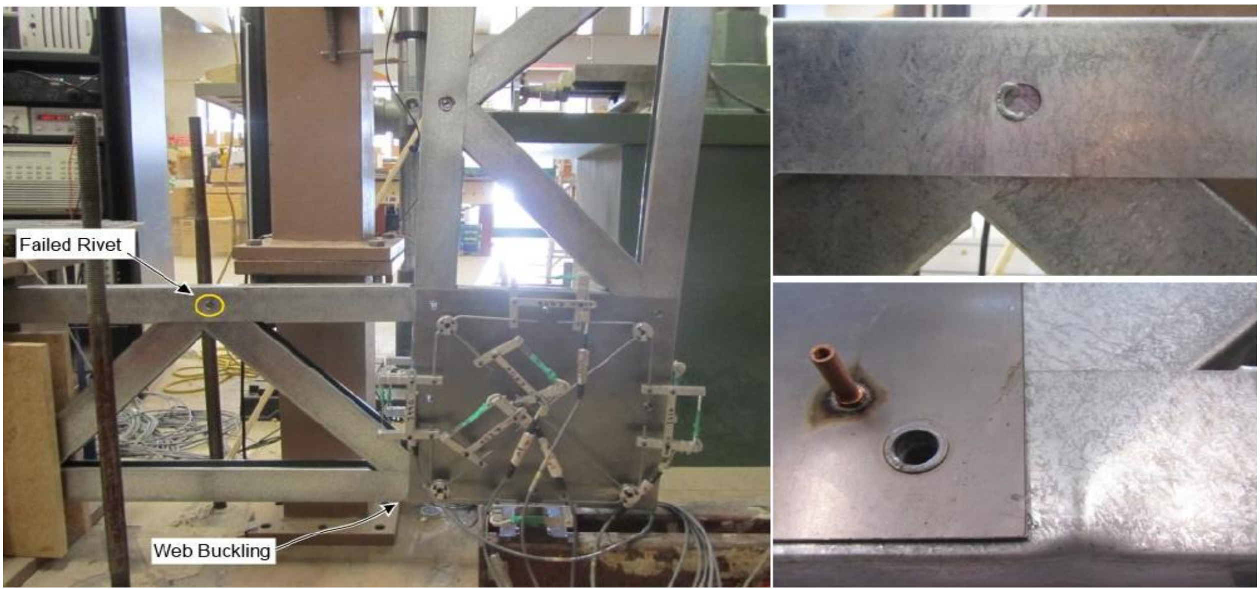

Fig. 18 Failed specimen in first moment connection test (left) with the failed rivet (top right) and buckled web (bottom right) highlighted

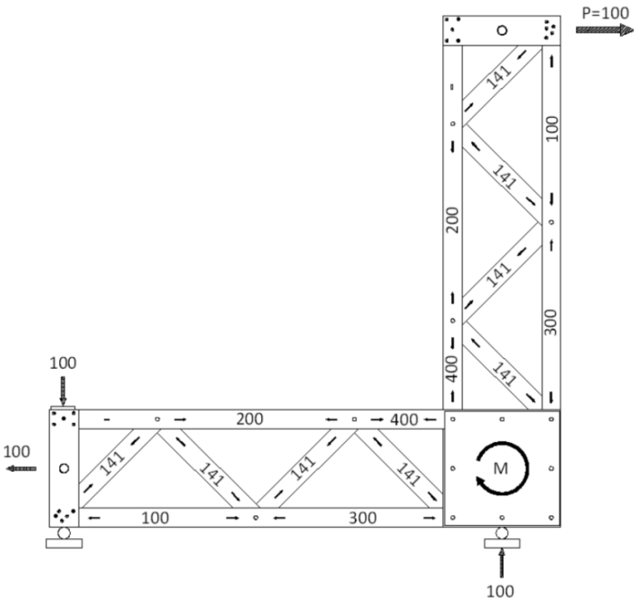

Fig. 19 Relative forces in moment connection specimen for an applied force of 100 units for an opening moment

the gusset plate using bolt group theory and was calculated as follows:

The vertical and horizontal force vectors acting on a particular rivet from the applied moment, R_{mx} and R_{my}, respectively are

$$R_{mx} = \frac{My}{\sqrt{\sum(x^2 + xy^2)}} \tag{4}$$

$$R_{my} = \frac{Mx}{\sqrt{\sum(x^2 + xy^2)}} \tag{5}$$

Where:

M is internal moment in the connection (equal to 1.49P)

y and x are distances from the centroid of the connecter group to the rivet.

The applied shear on the connection was equal to 100 units, which was divided equally among the rivets. The shear forces in each direction, R_{vx} and R_{vy} were added to the moment derived forces in each direction respectively before determining the magnitude, V and direction, θ of the resulting force using Eqs. (6) and (7), respectively

$$V = \sqrt{[(R_{mx} + R_{vx})^2 + (R_{my} + R_{vy})^2]} \tag{6}$$

$$\theta = tan^{-1}\left[\frac{(R_{mx} + R_{vx})}{(R_{my} + R_{vy})}\right] \tag{7}$$

The highest force was applied at the corners of the connection, which is expected, as these are the furthest from the centroid. The critical force of 1.14 P is lower than the forces acting through the rivets in the truss, which is why rivet shear failure was not observed to occur within the gusset.

3.2 Test 2 (*Cyclic behaviour of the moment connection*)

The main objective of this test was to determine the cyclic behaviour of the moment connection with HRCs. This was achieved by firstly loading the connection to yield in both opening and closing moments and noting the deflection, which occurred. Multiples of this deflection, μ were then targeted which indicates the available ductility in the connection. The results from the test are shown in Fig. 21.

The test specimen was firstly loaded in an opening moment until an elastic limit of 9.3 kNm was achieved. The

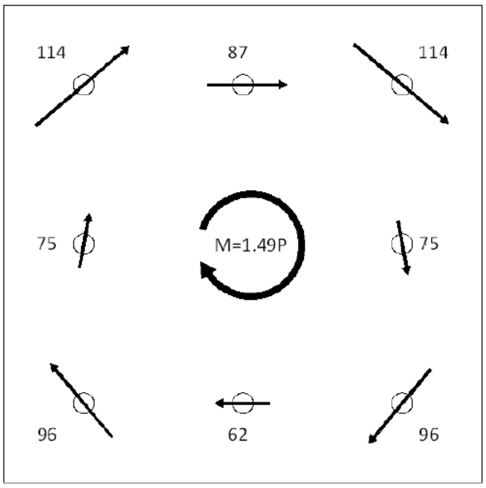

Fig. 20 Theoretical force vectors acting through HRCs in the gusseted moment connection with an applied force of 100 units for an opening moment

test was then loaded in a closing moment until an elastic limit of 6.5 kNm. After this, the specimen was loaded to a displacement of 1.25 times the displacement reached at the elastic limit for both the opening and closing moment. An attempt was then made at loading the specimen in a closing moment to a displacement of 2 times the elastic limit. Sideways buckling failure at the critical point in the compression chord of the bottom member occurred similar to what was observed in the first test specimen at a moment of 8.0 kNm. Failure modes are shown in Fig. 22. Local buckling in the tension chord of the bottom truss nearest to the gusset plate connection occurred.

The load capacity of the connection in a closing moment was unlikely to increase without significant damage to the specimen. Therefore, the rest of the test cycles were performed on an opening moment. The specimen was pulled until a displacement of two times the elastic limit was reached. A small amount of slip can be seen in the loading curve, which is due to permanent inelastic deformation of the rivets from when they were loaded to 1.25 times their elastic capacity. Although there is a small degree of slip, once the rivets begin to bear fully, the load profile acted elastically.

The specimen was then loaded and unloaded to two times the elastic limit three times. Each of these test cycles follow the same load profile and clearly show the same connection softening behaviour with more slip due to the extra displacement reached. A displacement of three times the elastic limit was intended for the final test before an ultimate moment of 14.5 kNm was reached. The failure mode was simultaneous rivet shear in all truss connections similar to the first test specimen.

3.3 Test 3 (Performance of the gusseted moment connection)

The results from the former two tests showed that when subjected to a closing moment the strength and behaviour of the connection is limited by the capacity of the chord member, which has been cut to allow intersecting truss

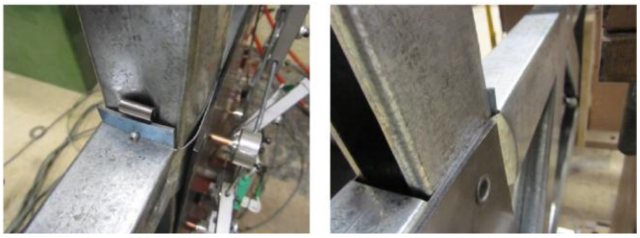

Fig. 22 Sideways buckling failure of the compression chord

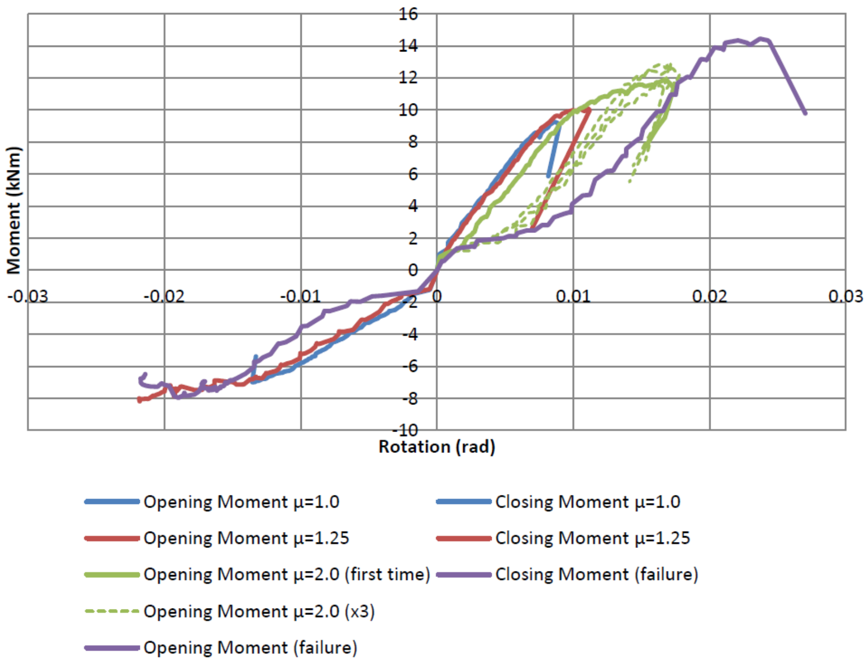

Fig. 21 Moment connection test result

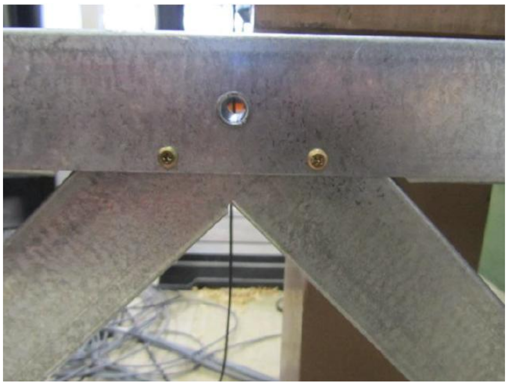

Fig. 23 Tek screws installed on either side of rivets in final moment connection test

Fig. 25 Net section fracture of tension member in third moment connection test

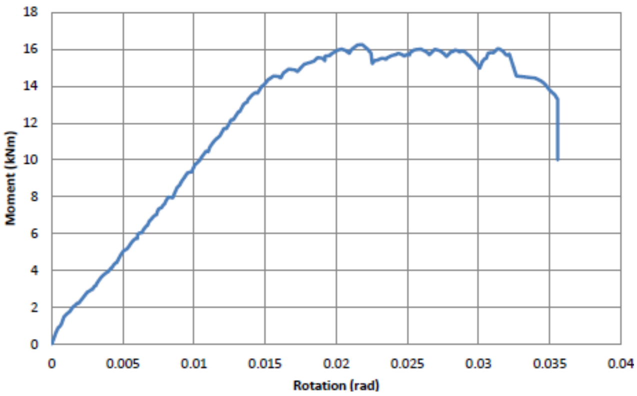

Fig. 24 Behaviour of the moment connection

members through. In an opening moment, the rivets consistently shear simultaneously until ultimate failure is reached in one of the connections. The focus of the final moment connection test was on the performance of the gusseted moment connection itself. Tek screws were installed either side of each rivet in the truss members (see Fig. 23) as this has been shown Mathieson *et al.* (2016) to increase the capacity of the connection.

The final moment connection test was only loaded a single time to failure in an opening moment. The result from the testing is plotted in Fig. 24 and show that the test remained elastic up to a moment of about 14 kNm. After the elastic limit was reached, it was observed that the rivets in the truss members were beginning to soften slightly at around the same time that the rivets in the gusseted connection also began to shear. Local buckling around the riveted connections was observed where the screws were connected similar to the equivalent test conducted for this study. Ultimate failure occurred at a moment of 16.3 kNm as net section fracture of the tension member in the bottom truss (see Fig. 25). It should be noted that this fracture goes through the whole section on both sides.

4. Theoretical failure loads and recommendations

One of the objectives of testing the moment connection was to determine whether the failure loads and loading patterns could be predicted based on force equilibrium and calculations. The results from this section will aid in discussing variations to the connection and support the future design of moment connections using gusseted interconnecting trusses. The focus of the first part of this section is only on tests with opening moments and a simple method of avoiding premature failure in a closing moment is presented afterwards.

4.1 Opening moment

In the first and second test, the primary failure mechanism was shearing of the rivet connectors at a maximum moment of 15.5 kNm and 14.5 kNm, respectively. An expected peak applied load for the moment connection failing in rivet shear can be derived by dividing the average T-joint test result by 2 (see Fig. 19). This can be converted to a maximum expected moment by multiplying by a factor of 1.49. Table 5 compares the results of the moment connection tests with the peak load expected based on T-joint test results.

As shown in Table 5, the failure load for the rivets outside of the gusset of the moment connection are higher than what was determined by T-joint testing. In the truss testing where the proposed reason for the discrepancy was an increased capacity for internal energy due to a longer rivet shank length. The suggested 'truss connection factor' which allows a strength increase of 25% for rivet shear in truss connections with three members was justified for both moment connection tests.

In the final test, ultimate failure occurred as net section fracture in the tension chord of the bottom truss. In this

Table 5 Comparison of failure loads for 12.7 × 0.95 mm rivets

Moment connection test	Average peak moment from test (kNm)	Average peak load T-joint test (kN)	Expected peak moment (kNm)	Difference between actual and expected
Elastic capacity	15.5	15.49	11.54	34%
Buckling failure	14.5	-	11.54	26%

member the section had its lips and web cut to allow an intersecting member to pass through as well as holes in the middle for the connecting rivet. The failure load for a section in net tension fracture (N^*), can be calculated from AS/NSZ4600 (2005) using Eq. (8).

$$N^* = 0.85\ k_t\ A_g\ f_u \tag{8}$$

Where:

k_t is net section efficiency factor, taken as 1.0 for this truss section

A_g is cross-sectional area of the section

f_u is ultimate strength of the material

The cross-sectional area is equal to 87.4 mm considering the reduction in area due to web and lip cuts and rivet holes, therefore the ultimate strength at failure was theoretically calculated from Eq. (8) as follows

$$N^* = 0.85 \times 87.4 \times 0.66 = 49 \text{ kN}$$

The expected failure load from Fig. 19 was 43.8 kN, which is 12% lower than the theoretical actual load. The factor of 0.85 is intended to take account sudden brittle failure, which was observed in the final test. An in-depth analysis of current design and proposed equations was used to calculate the capacity of CFS sections in tension is presented by Teh and Yazici (2013). In this paper it is shown that the current method used in AS/NZS 4600 (2005) consistently over predicts the capacity of CFS in net section fracture. Based on the mean value of $N^*/A_g f_u$, from the experimental testing on back-to-back channel sections performed by Teh and Yazici (2013), where the net section efficiency factor is unity as with the truss test in this paper, results would suggest that a factor of 0.75 better fits the data than 0.85. If 0.75 was used in Eq. (8), the expected failure load would be 43.3 kN which is within 2% of the expected failure load.

Significant squashing of the HRCs inside the gusseted connection was observed and is shown in Fig. 26, where

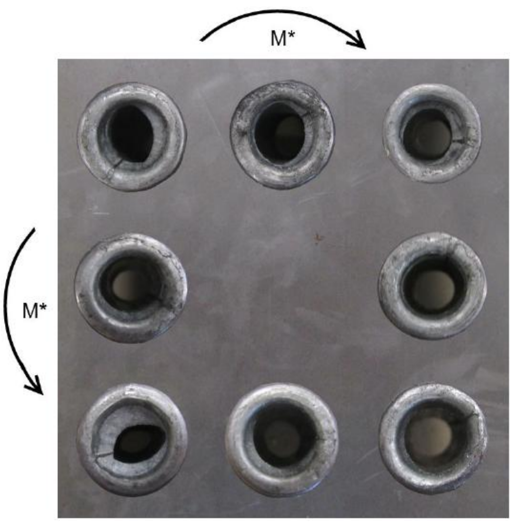

Fig. 26 HRCs after ultimate failure load for gusseted moment connection test

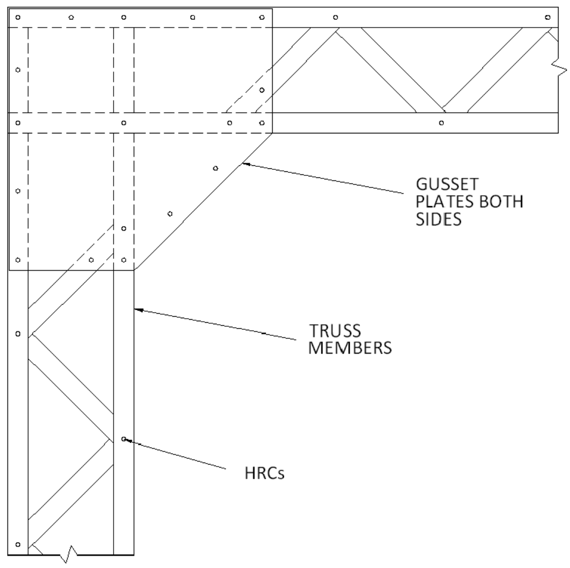

Fig. 27 Proposed extended gusset moment connection

the failed rivets are presented in the same arrangement as in Fig. 20. It appears that the most significant shearing occurred in the bottom left rivet; however, the degree of squashing is reasonably uniform around the rivets. Redistribution of stresses due to inelastic deformation in the corner rivets would have allowed the other rivets between corners to soften. From the force equilibrium as shown in Fig. 20, and the average ultimate rivet shear load of 20.13 kN from the previous two moment connection tests, the expected moment resulting in failure of the critical corner rivet would have been 17.1 kNm. This value is close to the actual ultimate failure moment of 16.5 kNm, which suggests the rivets inside the gusseted connection were on the verge of ultimate shear failure or had already started to fail.

4.2 Closing moment

It was determined from the first and second tests conducted that the strength of the assembly is limited by the buckling strength of the compression chord closest to the gusset, which was cut to allow intersecting members through. The HRCs work effectively at carrying moment. HRCS also shear across a gusseted connection. The gussets could therefore be extended out past the critical chord section to meet at the next intersecting connection. An example of this proposed connection is shown in Fig. 27.

This study proposed moment connection with an extended gusset; HRCs are aligned around the perimeter of the gusset to maximize the moment capacity and to increase the stability of the gusset section which is outset from the corner of the trusses. A rivet is provided in the center to hold the intersecting chord members together and to provide stability to the center of the gusset.

In terms of HRC to be used in bolted Tee-stubs, design recommendations were proposed by Ahmadi *et al*. (2016), as the current design guidelines by AISI (2012) could not predict the bearing strength of HRC in bolted Tee-stubs accurately. It was recommended to use a minimum end distance of 1.5 times the diameter of HRC.

For the HRC Tee-stubs, the following Eq. (9) was used to calculate the bearing strength of such connections

$$P_{b_t HRC} = n m_f \, C_{HRC} \, d_{HRC} \, t_{ply} \, F_u$$
$$0.75 \leq \; t_{ply\,.nom} \; \leq 1.15; 11 \; < \frac{d_{HRC}}{t_{ply}} < 22 \qquad (9)$$

Where

$m_f = 1$,
$C_{HRC} = 95 + 1.88 / (d/t)$

A reliability analysis was carried out in order to verify the validity of the proposed bearing equation. The proposed equation for the HRC Tee-stubs gave a test-to-predicted ratio, P_m, of 1.008 and reliability index, β, of 3.590, which is greater than the recommended reliability index of 3.5 as specified in AISI S100 (2012).

5. Conclusions

Traditional rigid moment connections using a group of connectors are not commonly provided for portal frames made from trusses, so a relatively novel method using HRCs has been developed and is presented in this paper. Results from both T-joints and truss assembly showed similar behavior; both in case of bearing and shear failure modes. The moment connections tested in this study used gussets on the outside as an alternative to putting additional members inside the connection. This reduces the amount of interconnecting elements and allowing multiple connectors to act as a group within the connection. The moment connections were tested in a perpendicular arrangement to allow for the greatest moment to shear or axial force ratio to be developed. Conclusions made from this study are as follows:

- In a closing moment the compression chord of the bottom truss failed in sideways buckling where it had been cut to allow an intersecting to pass through.
- In an opening moment, all HRCs in the truss members outside the gusseted connection failed simultaneously in shear.
- When 10 g Tek screws were provided around connections in the truss members, shear failure of the HRCs inside the gusset plate began to occur until the inside truss member in tension failed in net section fracture.
- Failure of the critical connections and members were shown to be predictable using force equilibrium, although current design provisions have been shown to be un-conservative for calculating net section fracture for CFS.
- The HRCs worked effectively at carrying moment across the non-extended gusseted connection but were less effective at transferring moment and shear. Therefore, an extended gusseted connection has been proposed. In the proposed moment connection with an extended gusset, HRCs are aligned around the perimeter of the gusset to maximize the moment capacity and to increase the stability of the gusset section, with local failure offset from within the connection region.

Acknowledgments

The financial support and provision of test materials from Howick Ltd., is gratefully acknowledged.

References

Ahmadi, A., Mathieson, C., Clifton, G.C., Das, R. and Lim, J.B.P. (2016), “An experimental study on a novel cold-formed steel connection for light gauge open channel steel trusses”, *J. Constr. Steel Res.*, **122**, 70-79. https://doi.org/10.1016/j.jcsr.2016.02.007

American Iron and Steel Institute (2012), North American specification for the design of cold-formed Steel Structural Members; NAS S100.

Australia/New Zealand Standard (AS/NZS) (2005), Cold-Formed Steel Structures, AS/NZS 4600:2005; Standards Australia/ Standards New Zealand.

Australia/New Zealand Standard (AS/NZS) (2002), Structural Design Actions, AS/NZS 1170:2002; Standards Australia/ Standards New Zealand.

Beena, K., Naveen, K. and Shruti, S. (2017), “Behaviour of bolted connections in concrete-filled steel tubular beam-column joints”, *Steel Compos. Struct., Int. J.*, **25**(4), 443-456. http://dx.doi.org/10.12989/scs.2017.25.4.443

Darcy, G. and Mahendran, M. (2008), “Development of a new cold-formed steel building system”, *Adv. Struct. Eng.*, **11**(6), 661-677. https://doi.org/10.1260/136943308787543621

Dundu, M. (2011), “Design approach of cold-formed steel portal frames”, *Int. J. Steel Struct.*, **11**(3), 259-273. https://doi.org/10.1007/s13296-011-3002-2

Kaitila, O., Kesti, J. and Makelainent, P. (2001), “The behaviour of a new type of connection system for light-weight steel structures applied to roof trusses”, *Steel Compos. Struct., Int. J.*, **1**(1), 17-32. http://dx.doi.org/10.12989/scs.2001.1.1.017

Li, D., Uy, B., Patel, V. and Aslani, F. (2017), “Analysis and design of demountable embedded steel column base connections”, *Steel Compos. Struct., Int. J.*, **23**(3), 303-315. http://dx.doi.org/10.12989/scs.2017.23.3.303

Lim, J.B.P. and Nethercot, D.A. (2004), “Finite element idealization of a cold-formed steel portal frame”, *J. Struct. Eng.*, **130**(1), 78-94. https://doi.org/10.1061/(ASCE)0733-9445(2004)130:1(78)

Mathieson, C., Clifton, G.C. and Lim, J.B.P. (2016), “Novel pin-jointed connection for cold-formed steel trusses”, *J. Constr. Steel Res.*, **116**, 173-182. https://doi.org/10.1016/j.jcsr.2015.08.009

Mills, J.E. (2000), “Knee joints in cold-formed channel portal frames”, (R.A. Laboube and W.W. Yu Eds.), In: *Recent Research and Developments in Cold-Formed Steel Design and Construction*, pp. 577-592.

Mills, J.E. (2012), “Knee joints in cold-formed channel portal frames: problems and pitfalls”, *Austral. J. Struct. Eng.*, **13**(2), 191-202.

Mills, J.E. and Laboube, R. (2004), “Self-drilling screw joints for cold-formed channel portal frames”, *J. Struct. Eng.*, **130**(11), 1799-1806. https://doi.org/10.1061/(ASCE)0733-9445(2004)130:11(1799)

Nunez, E., Torres, R. and Herrera, R. (2017), "Seismic performance of moment connections in steel moment frames with HSS columns", *Steel Compos. Struct., Int. J.*, **25**(3), 271-286.
http://dx.doi.org/10.12989/scs.2017.25.3.271
Roy, K., Ting, T.C.H., Lau, H.H. and Lim, J.B.P. (2018a), "Nonlinear behaviour of back-to-back gapped built-up cold-formed steel channel sections under compression", *J. Constr. Steel Res.*, **147**, 257-276.
https://doi.org/10.1016/j.jcsr.2018.04.007
Roy, K., Ting, T.C.H., Lau, H.H. and Lim, J.B.P. (2018b), "Nonlinear behavior of axially loaded back-to-back built-up cold-formed steel un-lipped channel sections", *Steel Compos. Struct., Int. J.*, **28**(2), 233-250.
http://dx.doi.org/10.12989/scs.2018.28.2.233
Roy, K., Ting, T.C.H., Lau, H.H. and Lim, J.B.P. (2018c), "Effect of thickness on the behaviour of axially loaded back-to-back cold-formed steel built-up channel sections - Experimental and numerical investigation", *Structures*, **16**, 327-346.
https://doi.org/10.1016/j.istruc.2018.09.009
Roy, K., Mohammadjani, C. and Lim, J.B.P. (2019), "Experimental and numerical investigation into the behaviour of face-to-face built-up cold-formed steel channel sections under compression", *Thin-Wall. Struct.*, **134**, 291-309.
https://doi.org/10.1016/j.tws.2018.09.045
Teh, L.H. and Yazici, V. (2013), "Shear lag and eccentricity effects of bolted connections in cold-formed steel sections", *Eng. Struct.*, **52**, 536-544.
https://doi.org/10.1016/j.engstruct.2013.03.024
Ting, T.C.H., Roy, K., Lau, H.H. and Lim, J.B.P. (2018), "Effect of screw spacing on behavior of axially loaded back-to-back cold-formed steel built-up channel sections", *Adv. Struct. Eng.*, **21**(3), 474-487.
https://doi.org/10.1260/1369-4332.15.9.1623
Wrzesien, A., Lim, J.B.P. and Nethercot, D. (2012), "Optimum joint detail for a general cold-formed steel portal frame", *Adv. Struct. Eng.*, **15(9)**, 1623-1640.
https://doi.org/10.1260/1369-4332.15.9.1623

BU

Notations

A_g	Cross-sectional area of the section
CFS	Cold-formed steel
f_u	Ultimate strength of the material
G	Permanent loading
HRC	Howick Rivet Connector
k_t	Net section efficiency factor
L_{floor}	Length of floor truss
L_{portal}	Maximum portal span
M	Internal Moment in the connection
M_{floor}	Moment resisted by floor truss
M_{knee}	Bending moment at knee
ULS	Ultimate limit state
Q	Imposed loading
SLS	Serviceability limit state
ω_{rafter}	Load on the portal frame rafter (kN/m)
ω_{floor}	Load on floor truss (kN/m)
ω_{portal}	Load on portal frame (kN/m)